Electronic Supplementary Material (ESI) for Inorganic Chemistry Frontiers.

Supporting Information for

Diversifying luminescence of phenanthro-diimine ligands in zinc complexes

*Diana Temerova,[a] Kristina S. Kisel,[a,b] Toni Eskelinen,[a] Alexei S. Melnikov,[c] Niko Kinnunen,[a] Pipsa Hirva,[a] Julia R. Shakirova,[b] Elena V. Grachova,[b] Igor O. Koshevoy[a]**

[a] Department of Chemistry, University of Eastern Finland, Joensuu, 80101, Finland

[b] St.Petersburg State University, Department of Chemistry, Universitetskii pr. 26, 198504, St.Petersburg, Russia.

[c] Centre for Nano- and Biotechnologies, Peter the Great St. Petersburg Polytechnic University, 195251 St. Petersburg, Russia.

E-mail: igor.koshevoy@uef.fi

Experimental section

General comments. 9,10-Dibromoanthracene,[1] 1-phenyl-2-(pyridin-2-yl)-1*H*-phenanthro[9,10-*d*]imidazole (**L1**)[2] and 1-(4-(anthracen-9-ylethynyl)phenyl)-2-(pyridin-2-yl)-1*H*-phenanthro[9,10-*d*]imidazole (**L2**)[2] were synthesized according to published procedures. Other reagents were used as received. Infrared spectra were measured on a Shimadzu IRAffinity-1 FTIR spectrophotometer in pressed KBr pellets. The solution ^{1}H and ^{1}H–^{1}H COSY NMR spectra were recorded on a Bruker AMX-400 spectrometer. Microanalyses were carried out in the analytical laboratory of the University of Eastern Finland.

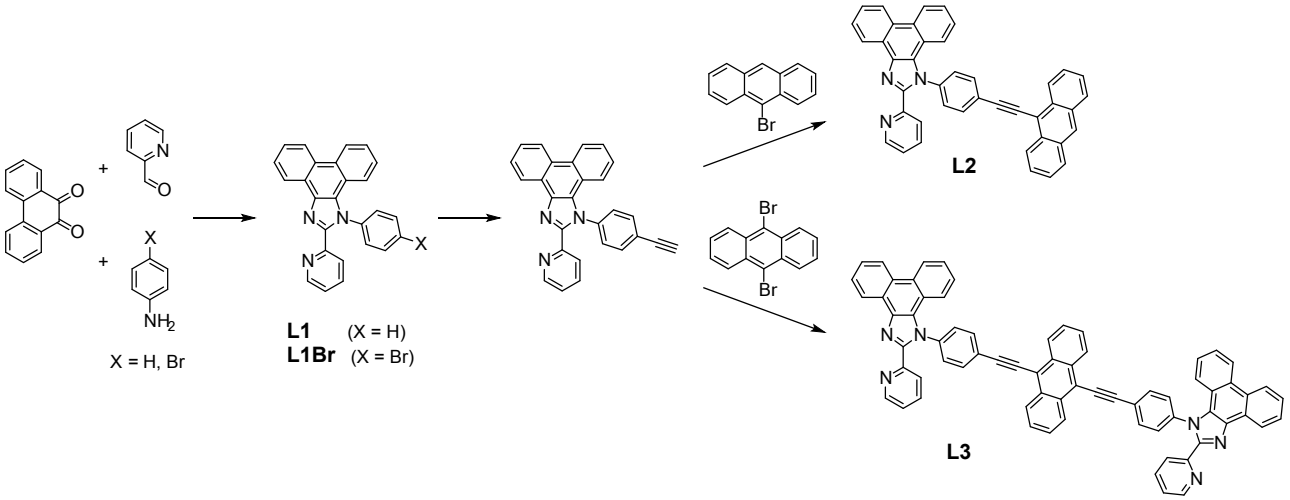

Scheme S1. Synthesis of ligands **L1**–**L3**.

9,10-Bis((4-(2-(pyridin-2-yl)-1*H*-phenanthro[9,10-*d*]imidazole-1-yl)phenyl)ethynyl)anthracene (L3). A mixture of 1-(4-ethynylphenyl)-2-(pyridin-2-yl)-*H*-phenanthro[9,10-*d*]imidazole[2] (200 mg, 0.5 mmol), 9,10-dibromoanthracene (85 mg, 0.25 mmol) and triphenylphosphine (68 mg, 0.2 mmol) in *n*-propylamine (15 mL) was degassed by three freeze-pump-thaw cycles. Bis(dibenzylideneacetone)palladium(0) (30 mg, 0.03 mmol) and copper(I) iodide (22 mg, 0.12 mmol) were added and the reaction mixture was stirred for 16 hours at 60°C under a nitrogen atmosphere. The resulting suspension was cooled to room temperature, the orange precipitate was collected, washed with *n*-propylamine (5 mL), methanol (5 mL), diethyl ether (5 mL) and dried (190 mg, 79%). Subsequent recrystallization at room temperature by a gas-phase diffusion of pentane into a dichlorobenzene solution afforded orange-red microcrystalline material (**L3_r**). Slow evaporation of chloroform-dichlorobenzene solution at +5 °C afforded yellow flaky material (**L3_y**). The yellow crystals of the minor form **L3_y$_{cr}$** suitable for XRD analysis were obtained at room temperature by a gas-phase diffusion of pentane into a dichlorobenzene-dichloromethane (1:5 volume mixture) solution of **L3**. ^{1}H NMR ($CDCl_3$, 298 K; δ): 8.92 (d, J_{HH} 7.9 Hz, 2H), 8.84−8.81 (m, 6H), 8.75 (d,

J_{HH} 8.1 Hz, 2H), 8.45 (m, 2H), 8.27 (d, J_{HH} 7.9 Hz, 2H), 8.01 (d, J_{HH} 8.4 Hz, 4H), 7.82−7.67 (m, 14H), 7.58 (m, 2H), 7.41−7.35 (m, 4H), 7.23 (m, 2H). ESI$^+$ MS (m/z): $[M+H]^+$ 965.34 (calcd. 965.34). Anal. Calcd for $C_{70}H_{40}N_6$ (red): C, 87.11; H, 4.18; N, 8.71. Found: C, 87.43; H, 4.10; N, 8.39. Anal. Calcd for $C_{70}H_{40}N_6$ (yellow): C, 87.11; H, 4.18; N, 8.71. Found: C, 87.26; H, 4.32; N, 8.42.

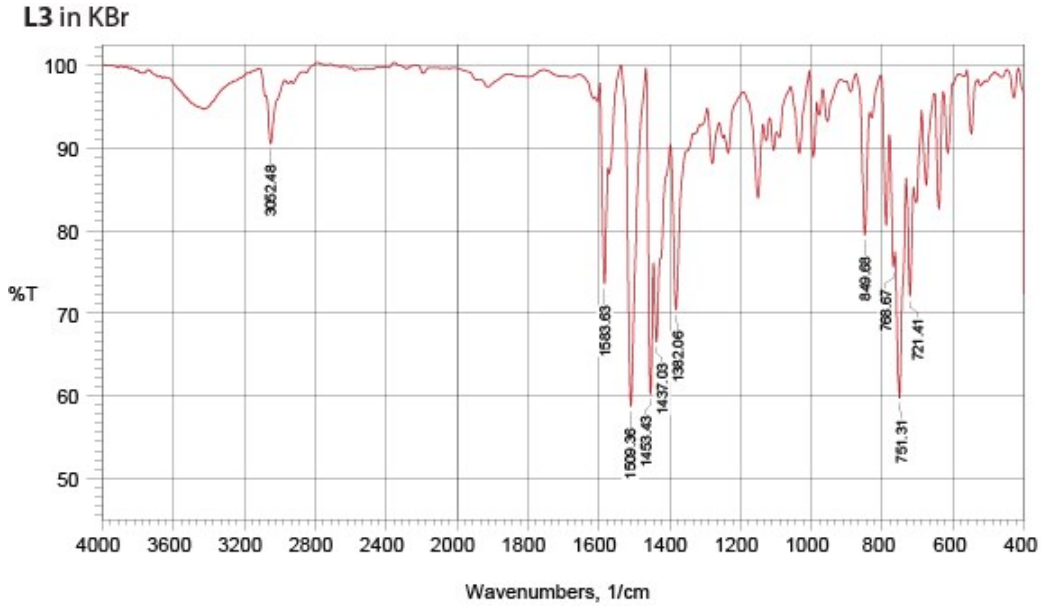

Zn(L1)Cl$_2$ (1Cl). A solution of **L1** (50 mg, 0.13 mmol) in dichloromethane (5 mL) was added to a solution of $ZnCl_2$ (18 mg, 0.13 mmol) in methanol (3 mL). The reaction mixture was stirred for 2 hours at room temperature to give a pale-yellow suspension. The precipitate was collected, washed with diethyl ether, and dried. The solid residue was recrystallized by a gas-phase diffusion of diethyl ether into a dichloromethane/methanol (form 1) or a chloroform/methanol (form 2) solution of **1Cl** at room temperature to give pale yellow crystalline material (64 mg, 94%, form 2). ^{1}H NMR ($CDCl_3$, 298 K; δ): 9.04 (d, J_{HH} 8.2 Hz, 1H), 8.91 (d, J_{HH} 4.6 Hz, 1H), 8.79 (d, J_{HH} 8.4 Hz, 1H), 8.72 (d, J_{HH} 8.4 Hz, 1H), 8.00−7.90 (m, 4H), 7.81−7.73 (m, 4H), 7.66−7.59 (m, 2H), 7.30 (m, 1H), 7.01 (d, J_{HH} 8.4 Hz, 1H), 6.75 (d, J_{HH} 8.3 Hz, 1H). Anal. Calcd for $C_{26}H_{17}Cl_2N_3Zn{\cdot}CH_2Cl_2$ (**1Cl_a** dichloromethane solvate, form 1): C, 54.72; H, 3.23; N, 7.09. Found: C, 55.01; H, 3.31; N, 7.26. Anal. Calcd for $C_{26}H_{17}Cl_2N_3Zn{\cdot}0.5CHCl_3$ (**1Cl_b** chloroform solvate, form 2): C, 56.09; H, 3.11; N, 7.40. Found: 56.26; H, 3.16; N, 7.45.

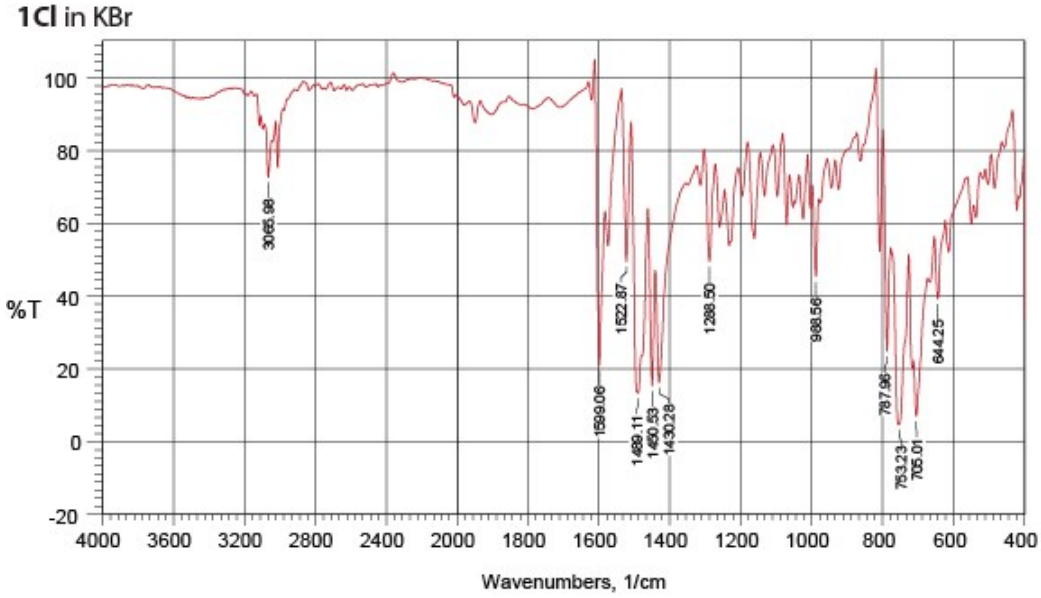

Zn(L1)I_2 (1I). A solution of **L1** (50 mg, 0.13 mmol) in dichloromethane (5 mL) was added to a suspension of ZnI_2 (43 mg, 0.13 mmol) in diethyl ether (7 mL). The resulting mixture turned transparent yellowish solution, which was stirred for 2 hours at room temperature to give a pale-yellow suspension. The precipitate was collected, washed with diethyl ether and dried. The solid residue was recrystallized by a gas-phase diffusion of diethyl ether into a dichloromethane (form 1) or a chloroform (form 2) solution of **1I** at room temperature to give pale yellow crystalline material (90 mg, 97%, form 2). ^{1}H NMR ($CDCl_3$, 298 K; δ): 9.20 (d, J_{HH} 8.2 Hz, 1H), 8.92 (d, J_{HH} 4.7 Hz, 1H), 8.79 (d, J_{HH} 8.4 Hz, 1H), 8.72 (d, J_{HH} 8.4 Hz, 1H), 8.00−7.90 (m, 4H), 7.82−7.73 (m, 4H), 7.66−7.59 (m, 2H), 7.30 (m, 1H), 7.01 (d, J_{HH} 8.4 Hz, 1H), 6.71 (d, J_{HH} 8.3 Hz, 1H). Anal. Calcd for $C_{26}H_{17}I_2N_3Zn$ (dichloromethane solvate, form **1I_a**): C, 45.22; H, 2.48; N, 6.08. Found: C, 44.93; H, 2.48; N, 6.11. Anal. Calcd for $C_{26}H_{17}I_2N_3Zn$ (solvent free form **1I_b**): C, 45.22; H, 2.48; N, 6.08. Found: C, 45.33; H, 2.66; N, 5.85.

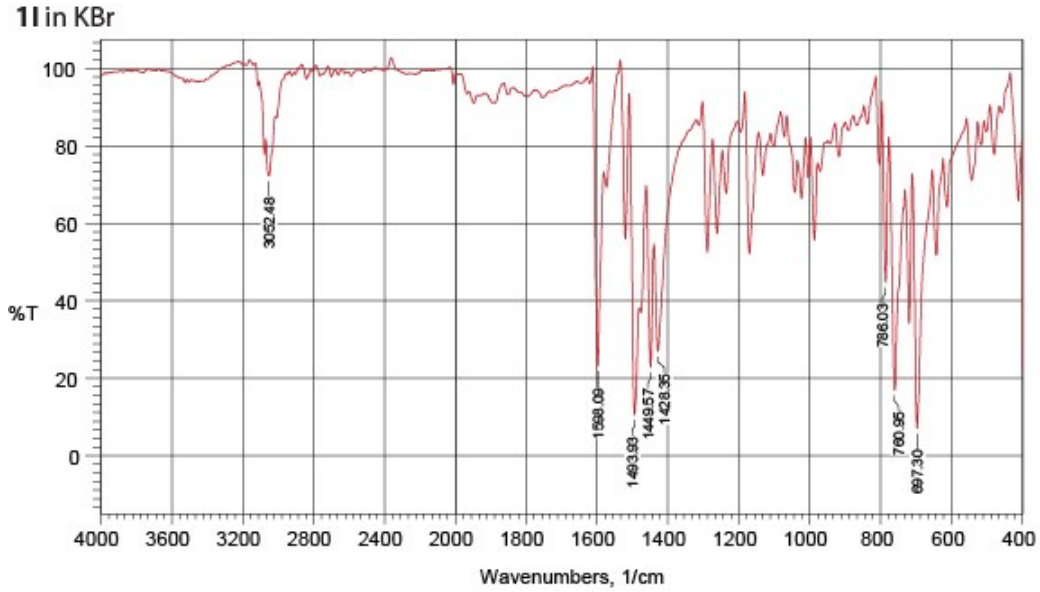

Zn(L1)(OAc)$_2$ (1OAc). Prepared similarly to **1Cl** using $Zn(OAc)_2{\cdot}2H_2O$ (30 mg, 0.13 mmol) instead of $ZnCl_2$ to give a clear pale yellow solution. After removing the solvent under reduced pressure, the residue was recrystallized by a gas-phase diffusion of diethyl ether into a chloroform solution of **1OAc** at room temperature to give pale yellow crystalline material (64 mg, 80%). ^{1}H NMR ($CDCl_3$, 298 K; δ): 9.18−9.13 (m, 2H), 8.78 (d, J_{HH} 8.4 Hz, 1H), 8.70 (d, J_{HH} 8.3 Hz, 1H), 7.97−7.85 (m, 4H), 7.79−7.72 (m, 3H), 7.68 (t, J_{HH} 7.9 Hz, 1H), 7.61 (t, J_{HH} 7.7 Hz, 1H), 7.53 (m, 1H), 7.30 (m, 1H), 7.01 (d, J_{HH} 8.3 Hz, 1H), 6.70 (d, J_{HH} 8.2 Hz, 1H), 2.09 (s, 6H). Anal. Calcd for $C_{30}H_{23}O_4N_3Zn$: C, 64.93; H, 4.18; N, 7.57. Found: C, 64.86; H, 4.31; N, 7.53.

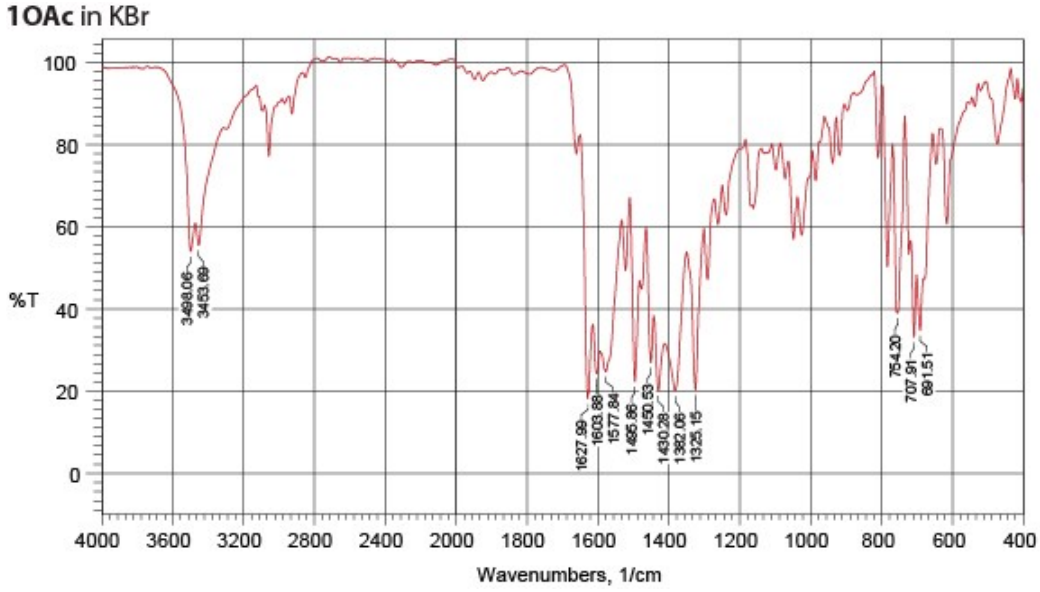

Zn(L2)Cl$_2$ (2Cl). A solution of **L2** (50 mg, 0.09 mmol) in dichloromethane (5 mL) was added to a solution of $ZnCl_2$ (12 mg, 0.09 mmol) in methanol (3 mL). The reaction mixture was stirred for 30 minutes at room temperature to give a yellow suspension. The precipitate was collected, washed with diethyl ether and dried. The solid residue was recrystallized by a gas-phase diffusion of pentane into a dichloromethane solution of **2Cl** at room temperature to give yellow crystalline material (58 mg, 93%). ^{1}H NMR ($CDCl_3$, 298 K; δ): 9.06 (d, J_{HH} 8.2 Hz, 1H), 8.93 (d, J_{HH} 4.7 Hz, 1H), 8.82 (d, J_{HH} 8.4 Hz, 1H), 8.74 (m, 3H), 8.59 (s, 1H), 8.28 (d, J_{HH} 8.4 Hz, 2H), 8.12 (d, J_{HH} 8.4 Hz, 2H), 7.95 (t, J_{HH} 7.4 Hz, 1H), 7.91 – 7.79 (m, 4H), 7.74 – 7.59 (m, 6H), 7.42 (t, J_{HH} 7.8 Hz, 1H), 7.22 (d, J_{HH} 8.3 Hz, 1H), 6.95 (d, J_{HH} 8.2 Hz, 1H). Anal. Calcd for $C_{42}H_{25}Cl_2N_3Zn$: C, 71.25; H, 3.56; N, 5.94. Found: C, 70.84; H, 3.56; N, 5.95.

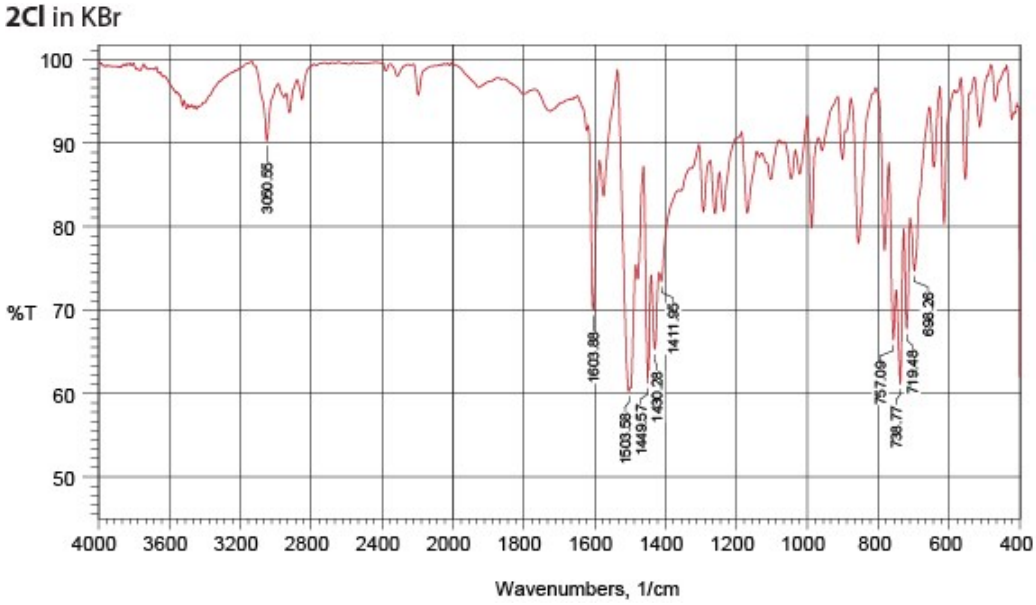

Zn(L2)I_2 (2I). A solution of **L2** (50 mg, 0.09 mmol) in dichloromethane (5 mL) was added to a suspension of ZnI_2 (28 mg, 0.09 mmol) in diethyl ether (7 mL). The resulting solution was stirred for 30 minutes at room temperature to give a yellow suspension. The precipitate was collected, washed with diethyl ether and dried. The solid residue was recrystallized by a gas-phase diffusion of diethyl ether into a chloroform/methanol solution of **2I** at room temperature to give orange crystalline material (75 mg, 96%). ^{1}H NMR ($CDCl_3$, 298 K; δ): 9.22 (d, J_{HH} 8.1 Hz, 1H), 8.95 (d, J_{HH} 5.0 Hz, 1H), 8.82 (d, J_{HH} 8.4 Hz, 1H), 8.74 (m, 3H), 8.59 (s, 1H), 8.28 (d, J_{HH} 8.2 Hz, 2H), 8.12 (d, J_{HH} 8.3 Hz, 2H), 7.96 (t, J_{HH} 7.4 Hz, 1H), 7.89 – 7.80 (m, 4H), 7.73 – 7.59 (m, 6H), 7.42 (t, J_{HH} 7.8 Hz, 1H), 7.22 (m, 1H), 6.94 (d, J_{HH} 8.3 Hz, 1H). Anal. Calcd for $C_{42}H_{25}I_2N_3Zn{\cdot}0.5CHCl_3$: C, 53.70; H, 2.70; N, 4.2. Found: C, 53.95; H, 2.88; N, 4.46.

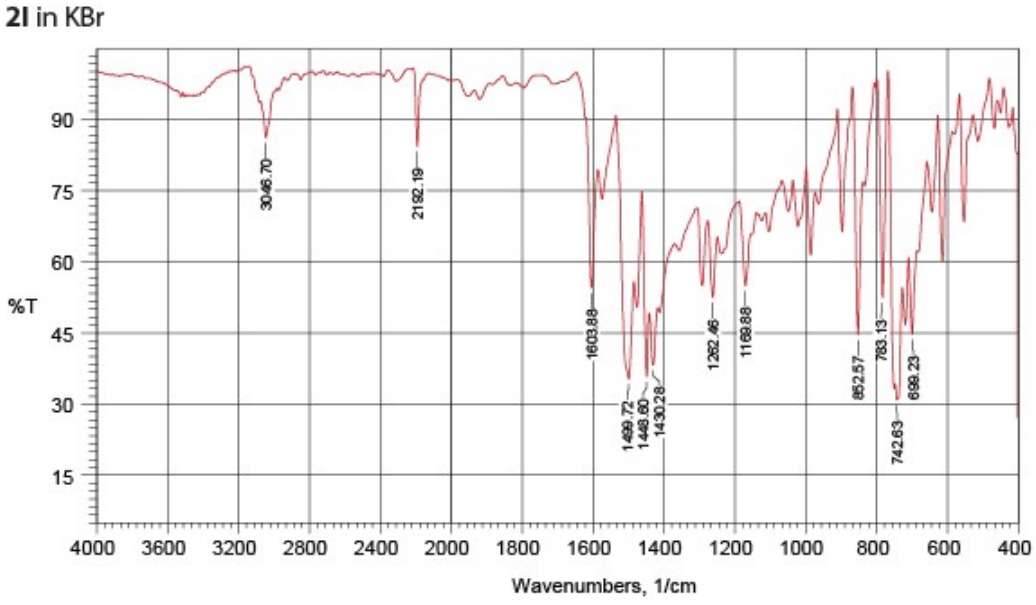

Zn(L2)(OAc)$_2$ (2OAc). Prepared similarly to **2Cl** using $Zn(OAc)_2{\cdot}2H_2O$ (19 mg, 0.09 mmol) instead of $ZnCl_2$ to give a clear yellow solution. After removing the solvent under reduced pressure, the residue was recrystallized by a gas-phase diffusion of pentane into dichloromethane solution of **2OAc** at room temperature to give yellow microcrystalline material (54 mg, 82%). ^{1}H NMR ($CDCl_3$, 298 K; δ): 9.23−9.14 (m, 2H), 8.81 (d, J_{HH} 8.4 Hz, 1H), 8.75−8.71 (m, 3H), 8.58 (s, 1H), 8.23 (d, J_{HH} 8.2 Hz, 2H), 8.11 (d, J_{HH} 8.4 Hz, 2H), 7.97 (t, J_{HH} 7.4 Hz, 1H), 7.83 – 7.56 (m, 11H), 7.39 (t, J_{HH} 7.8 Hz, 1H), 7.22 (d, J_{HH} 8.2 Hz, 1H), 6.92 (d, J_{HH} 7.9 Hz, 1H), 2.09 (s, 6H). Anal. Calcd for $C_{46}H_{31}O_4N_3Zn{\cdot}CH_2Cl_2$: C, 67.20; H, 3.96; N, 5.00. Found: C, 67.41; H, 4.04; N, 5.17.

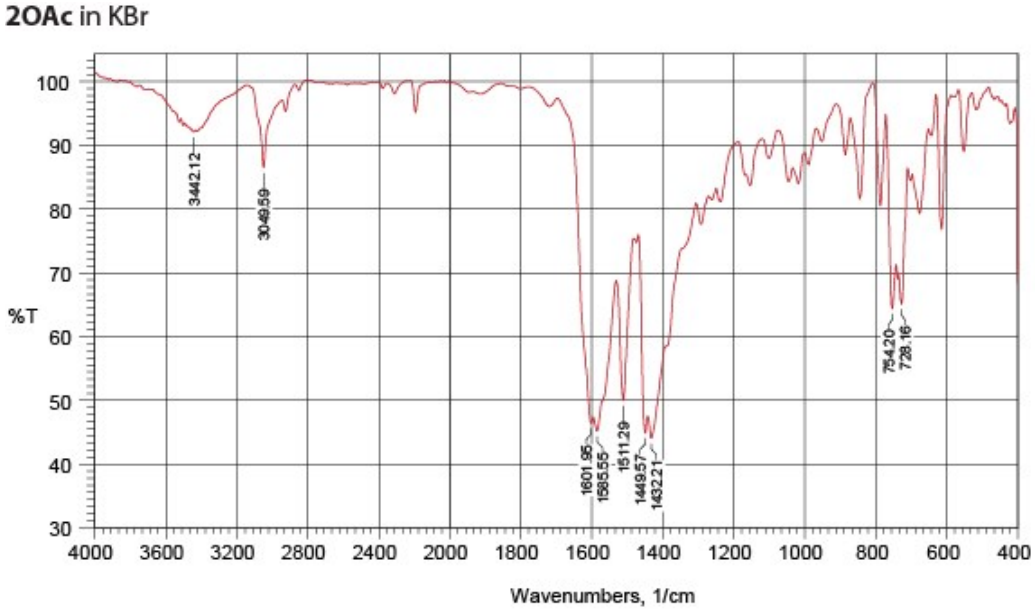

Zn$_2$(L3)(OAc)$_4$ (3OAc). A suspension of **L3** (50 mg, 0.05 mmol) in dichloromethane (7 mL) was treated with a solution of $Zn(OAc)_2{\cdot}2H_2O$ (23 mg, 0.10 mmol) in methanol (3 mL). The resulting mixture was stirred for 2 hours at room temperature to give a clear lemon-greenish solution. After removing the solvent under reduced pressure, the residue was dissolved in dichloromethane and separated into portions. Slow evaporation of a dichloromethane-ethanol solution of **3OAc** at room temperature afforded red microcrystalline material (**3OAc_r**). Gas-phase diffusion of pentane into a dichloromethane-methanol solution of **3OAc** at room temperature afforded yellow microcrystalline material (**3OAc_y**), total yield 52 mg (75%). The yellow crystals of the minor form **3OAc_y$_{cr}$** suitable for XRD analysis were obtained at room temperature by a slow evaporation of a chloroform-methanol solution of **3OAc** at +5 °C. ^{1}H NMR ($CDCl_3$, 298 K; δ): 9.23−9.14 (m, 4H), 8.86−8.82 (m, 6H), 8.73 (d, J_{HH} 8.1 Hz, 2H), 8.28 (m, 4H), 7.98 (m, 2H), 7.88−7.80 (m, 12H), 7.66 (m, 2H), 7.59 (m, 2H), 7.40 (m, 2H), 7.22 (m, 2H), 6.93 (d, J_{HH} 7.2 Hz, 2H), 2.10 (s, 12H). Anal. Calcd for $C_{78}H_{52}O_8N_6Zn_2{\cdot}CH_3OH$: C, 69.56; H, 4.14; N, 6.16. Found: C, 69.32; H, 4.12; N, 6.65.

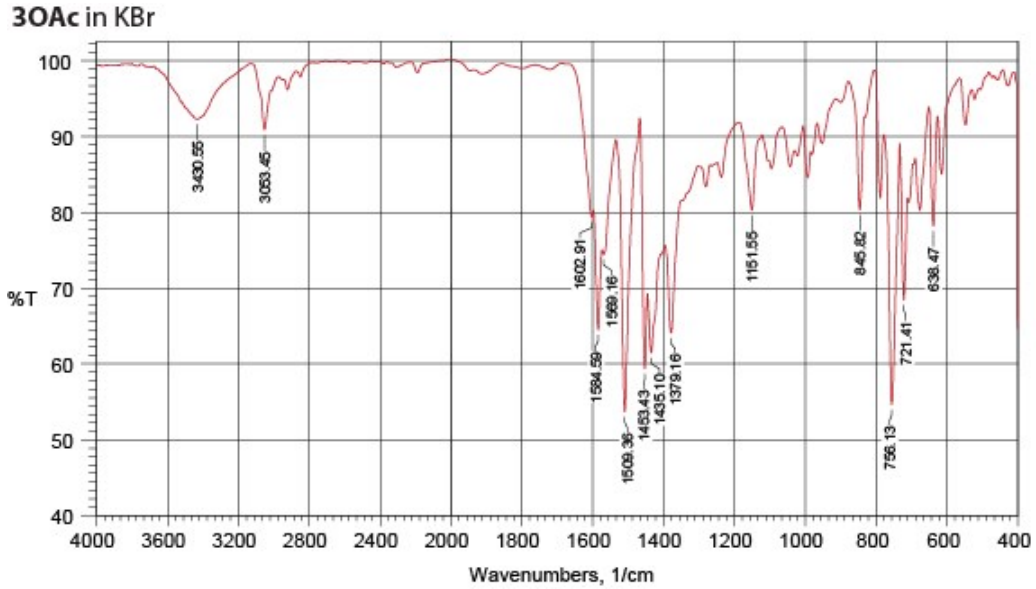

X-ray structure determinations and powder measurements. The crystals of **L3_y**, **1Cl**, **1I**, **1OAc**, **2Cl**, **2I**, **3OAc_y** were immersed in cryo-oil, mounted in a Nylon loop, and measured at a temperature of 150 K. The crystal of **1I** was also measured at variable temperature (210, 240, 270, 298 K). The X-ray diffraction data were collected with Bruker Kappa Apex II, Smart Apex II and Kappa Apex II Duo diffractometers using Mo Kα (λ = 0.71073 Å) radiation. The *APEX2*[3] program package was used for cell refinements and data reductions. A numerical or semi-empirical absorption correction (*SADABS*)[4] was applied to all data. The structures were solved by direct methods using the *SHELXS*-2018[5] program with the *WinGX*[6] graphical user interface. Structural refinements were carried out using *SHELXL*-2018.[5]

The crystallization solvent molecules in **L3**, **1OAc**, **2Cl**, **3OAc_y** could not be resolved unambiguously. The contribution of the missing solvent to the calculated structure factors was taken into account by using a *SQUEEZE* routine[7] of *PLATON*.[8] The missing solvent was not taken into account in the unit cell content. All non-H atoms were anisotropically refined, and all hydrogen atoms were positioned geometrically and constrained to ride on their respective parent atoms with C−H = 0.95–1.00 Å and U_{iso} = 1.2–1.5U_{eq} (parent atom). The crystallographic details are summarized in Table S1.

Powder XRD patterns were recorded with a Bruker Advance D8 and Rigaku Ultima IV diffractometers using Cu Kα (1.54184 Å) radiation source (Bruker: 40 kV/ 40 mA; Rigaku: 40 kV/ 30 mA). Divergence and receiving slits of 1.0 (Bruker) or 0.5 (Rigaku) mm were used together with Ni filter (Bruker) in the measurements. Prior to measurement, a sample was placed on a Si-single crystal zero background sample holder. The diffraction patterns were scanned from 5^0 to 90^0 (Bruker)

or 3^0 to 60^0 (Rigaku) in two theta scale using locked couple technique in Bragg-Brentano geometry. Collection time of 2 seconds was used together with a step size of 0.02^0 per step.

Photophysical Measurements. UV–vis absorption spectra were recorded on a Shimadzu UV-1800 spectrophotometer. The excitation and emission spectra in solution (1,2-dichloroethane, DCE) and in the solid state were recorded with a HORIBA FluoroMax-4 spectrofluorometer. The excited state lifetimes and the absolute photoluminescence quantum yields in the solid phase were performed on a HORIBA Scientific FluoroLog-3 spectrofluorometer using a HORIBA Quanta-phi integration sphere. Helium-nitrogen optical cryostat optCryo 105 with temperature control system were used for cooling the samples in the temperature range 78–295 K. A pulse laser DTL-399QT "Laser-export Co. Ltd" (351 nm, 50 mW, pulse width 6 ns, repetition rate 1 kHz), a monochromator MUM (LOMO, slit bandwidth 1 nm), photon counting head H10682 (Hamamatsu) and a multiple-event time digitizer P7887 (FAST ComTec GmbH) were used for lifetime measurements in the temperature range 78−295 K. The uncertainty of the quantum yield determinations was in the range of ±5% (an average of three replications, which correspond to different orientations of the sample). The emission quantum yield in solutions was determined by the comparative method using coumarin 102 in ethanol ($\Phi r = 0.764$)[9] with refraction indexes of dichloroethane and ethanol equal to 1.4448 and 1.3614, respectively. For measurement of the excited state lifetime of phosphorescence band for **1I**, argon gas was bubbled through the solution of **1I** in 1,2-dichloroethane ($c = 10^{-5}$ M) for 10 min. at room temperature for deaeration. The decay was monitored at 560 nm ($\lambda_{exc} = 351$ nm).

Computational details. Density functional theory calculations were performed with Gaussian 16[10] software package using the PBE0[11] hybrid functional and a D3-BJ[12-13] empirical dispersion correction. A def2-TZVPPD[14] basis set was used for the zinc and iodine atoms, while the lighter atoms were treated with a 6-311+G(d,p) basis set. All models were optimized without any constraints. Excited state structures were optimized with TD-DFT. Frequency calculations were also performed for each optimized structure to confirm the nature of the stationary points. Solvation effects were considered by running the calculations in a chloroform solvent using the C-PCM[15-16] solvation model, as implemented in Gaussian.

Table S1. Predicted (PBE0) low energy excitations for complexes **1X**–**3X** and **L3** in chloroform.

	Transition	λ_{calc}, nm	f	MO contribution
1Cl	$S_0 \rightarrow S_1$	372	0.62	99% HOMO→LUMO
	$S_0 \rightarrow S_2$	331	0.02	95% H-1 →LUMO
	$S_0 \rightarrow S_3$	307	0.02	43% HOMO→L+1, 40% HOMO →L+2
	$S_0 \rightarrow S_4$	299	0.06	51% HOMO→L+1, 37% HOMO →L+2
1I	$S_0 \rightarrow S_1$	376	0.54	98% HOMO→LUMO
	$S_0 \rightarrow S_2$	356	0.002	100% H-1→LUMO
	$S_0 \rightarrow S_3$	347	0.06	93% H-2→LUMO
	$S_0 \rightarrow S_4$	342	0.006	94% H-3→LUMO
1OAc	$S_0 \rightarrow S_1$	367	0.56	98% HOMO→LUMO
	$S_0 \rightarrow S_2$	321	0.01	82% H-1→LUMO, 10% HOMO→L+2
	$S_0 \rightarrow S_3$	310	0.02	40% HOMO→L+2, 36% HOMO→L+1
	$S_0 \rightarrow S_4$	310	0.02	93% H-2→LUMO
	$S_0 \rightarrow S_5$	299	0.06	53% HOMO→L+1, 35% HOMO →L+2
2Cl	$S_0 \rightarrow S_1$	451	0.65	99% HOMO→LUMO
	$S_0 \rightarrow S_2$	406	10^{-4}	99% HOMO→L+1
	$S_0 \rightarrow S_3$	374	0.61	97% H-1→L+1
2I	$S_0 \rightarrow S_1$	451	0.66	99% HOMO→LUMO
	$S_0 \rightarrow S_2$	407	$3 \cdot 10^{-4}$	99% HOMO→L+1
	$S_0 \rightarrow S_3$	376	0.52	94% H-1→L+1
	$S_0 \rightarrow S_4$	367	0.01	92% H-1→LUMO
2OAc	$S_0 \rightarrow S_1$	450	0.64	99% HOMO→LUMO
	$S_0 \rightarrow S_2$	384	0.002	99% HOMO→L+1
	$S_0 \rightarrow S_3$	378	0.12	85% H-1→LUMO, 13% H-1→L+1
	$S_0 \rightarrow S_4$	364	0.43	85% H-1→L+1, 12% H-1→LUMO
L3	$S_0 \rightarrow S_1$	524	1.38	99% HOMO→LUMO
3OAc	$S_0 \rightarrow S_1$	525	1.37	99% HOMO→LUMO

Table S2. Predicted (PBE0) emissions parameters for complexes **1X**–**3X** and **L3** in chloroform.

Complex	Transition	λ_{calc}, nm	E_{calc}, eV	f	Assignment
1Cl	$S_1 \rightarrow S_0$	425	2.9	0.694	ILCT/ππ*
1I		429	2.9	0.566	ILCT/ππ*
1I	$T_1 \rightarrow S_0$	681	1.8	-	ILCT/ππ*
1OAc	$S_1 \rightarrow S_0$	423	2.9	0.647	ILCT/ππ*
2Cl		521	2.4	0.658	ππ*
2I		521	2.4	0.668	ππ*
2OAc		520	2.4	0.651	ππ*
3OAc		607	2.0	1.381	ππ*
L3		607	2.0	1.388	ππ*

Table S3. Crystal data and structure refinement for ligand **L3**, and zinc complexes **1Cl**, **1I**, **1OAc**, **2Cl**, **2I**, **3OAc_y**.

Identification code	**L3_y$_{cr}$**	**1I_a**	**1Cl_a**	**1Cl_b**	**1OAc**	**2I**	**2Cl**	**3OAc_y**
CCDC	2060309	2060304	2060299	2060300	2060311	2060306	2060310	2060308
Empirical formula	$C_{70}H_{40}N_6$	$C_{27}H_{19}Cl_2I_2N_3Zn$	$C_{27}H_{19}Cl_4N_3Zn$	$C_{53}H_{35}Cl_7N_6Zn_2$	$C_{60}H_{48}N_6O_9Zn_2$	$C_{43}H_{26}Cl_3I_2N_3Zn$	$C_{42}H_{25}Cl_2N_3Zn$	$C_{78}H_{52}N_6O_8Zn_2$
Formula weight	965.08	775.52	592.62	1134.76	1127.78	1009.18	707.92	1331.99
Temperature (K)				150(2)				
Wavelength (Å)	0.71073	0.71073	0.71073	0.71073	0.71073	0.71073	0.71073	0.71073
Crystal system	Triclinic	Triclinic	Monoclinic	Orthorhombic	Triclinic	Orthorhombic	Monoclinic	Triclinic
Space group	$P\bar{1}$	$P\bar{1}$	$P2_1/c$	$Pbcn$	$P\bar{1}$	$Pna2_1$	$P2_1/c$	$P\bar{1}$
Unit cell dimensions								
a (Å)	8.8354(6)	8.9526(8)	11.9425(7)	31.926(3)	10.2600(19)	20.2544(13)	19.0446(19)	7.8436(11)
b (Å)	9.8627(7)	12.4604(11)	10.5173(7)	9.5574(7)	11.153(2)	15.5170(11)	10.5617(10)	16.577(3)
c (Å)	15.8345(11)	13.1177(11)	20.1014(13)	15.8596(10)	11.593(2)	12.0814(7)	20.9281(19)	16.591(2)
a (°)	90.013(2)	91.271(4)	90.000(0)	90.000(0)	74.507(6)	90.000(0)	90.000(0)	84.069(4)
β (°)	100.607(2)	105.489(4)	91.8770(10)	90.000(0)	76.974(7)	90.000(0)	94.074(3)	83.755(4)
γ (°)	91.344(2)	105.098(4)	90.000(0)	90.000(0)	80.014(6)	90.000(0)	90.000(0)	89.027(4)
Volume (Å^3)	1355.87(16)	1354.9(2)	2523.4(3)	4839.2(7)	1236.4(4)	3797.0(4)	4198.9(7)	2132.9(5)
Z	1	2	4	4	1	4	4	1
ρ_{calc} (Mg/m^3)	1.182	1.901	1.560	1.558	1.515	1.767	1.120	1.037
μ (mm^{-1})	0.070	3.404	1.419	1.423	1.039	2.520	0.741	0.611
F(000)	502	744	1200	2296	582	1968	1448	686
Crystal size (mm^3)	0.268 × 0.163 × 0.086	0.334 × 0.080 × 0.053	0.709 × 0.314 × 0.275	0.303 × 0.083 × 0.061	0.497 × 0.193 × 0.076	0.194 × 0.062 × 0.041	0.275 × 0.157 × 0.130	0.168 × 0.107× 0.038
θ range for data collection (°)	1.308 to 27.499	1.619 to 29.998	2.186 to 29.999	1.276 to 29.994	1.856 to 30.999	1.653 to 29.998	1.072 to 26.999	1.241 to 25.049

Index ranges	-11<=h<=11, -12<=k<=12, -20<=l<=20	-12<=h<=12, -17<=k<=17, -18<=l<=18	-16<=h<=11, -14<=k<=13, -26<=l<=28	-38<=h<=44, -13<=k<=13, -14<=l<=22	-14<=h<=14, -16<=k<=16, -16<=l<=16	-28<=h<=23, -17<=k<=21, -16<=l<=16	-24<=h<=24, -13<=k<=13, -26<=l<=26	-9<=h<=9, -19<=k<=19, -19<=l<=19
Reflections collected	40903	71811	25956	39007	54849	30183	68472	62081
Independent reflections	6231 [R(int) = 0.0525]	7921 [R(int) = 0.0687]	6790 [R(int) = 0.0189]	7035 [R(int) = 0.0529]	7867 [R(int) = 0.0654]	10315 [R(int) = 0.0386]	9080 [R(int) = 0.0531]	7521 [R(int) = 0.1314]
Completeness to θ = 25.242°	100.0 %	100.0 %	100.0 %	99.5 %	100.0 %	99.9 %	99.6	99.4 %
Absorption correction	Semi-empirical from equivalents	Numerical	Numerical	Numerical	Numerical	Semi-empirical from equivalents	Numerical	Numerical
Max. and min. transmission	0.994 and 0.982	0.840 and 0.396	0.696 and 0.433	0.918 and 0.672	0.925 and 0.626	0.904 and 0.641	0.822 and 0.741	0.977 and 0.904
Refinement method	Full-matrix least-squares on F^2							
Data/ restrains/ parameters	6231 / 0 / 343	7921 / 0 / 316	6790 / 0 / 316	7035 / 1 / 316	7867 / 0 / 354	10315 / 1 / 469	9080 / 81 / 404	7521 / 30 / 424
GOOF on F^2	1.020	1.033	1.035	1.049	1.043	1.021	1.135	1.055
Final R indices [$I>2\sigma(I)$][a]	R1 = 0.0542, wR2 = 0.1329	R1 = 0.0321, wR2 = 0.0748	R1 = 0.0332, wR2 = 0.0862	R1 = 0.0454, wR2 = 0.1039	R1 = 0.0450, wR2 = 0.0863	R1 = 0.0346, wR2 = 0.0657	R1 = 0.0940, wR2 = 0.1952	R1 = 0.1025, wR2 = 0.2040
R indices (all data)	R1 = 0.0878, wR2 = 0.1496	R1 = 0.0427, wR2 = 0.0815	R1 = 0.0399, wR2 = 0.0899	R1 = 0.0671, wR2 = 0.1137	R1 = 0.0671, wR2 = 0.0973	R1 = 0.0487, wR2 = 0.0703	R1 = 0.1189, wR2 = 0.2081	R1 = 0.1500, wR2 = 0.2233
Largest diff. peak and hole (e.Å^{-3})	0.666 and -0.226	2.030 and -1.157	1.152 and -1.542	0.955 and -0.926	0.784 and -0.841	0.873 and -0.580	0.945 and -1.350	0.533 and -0.433

[a] $R_1 = \Sigma||F_o| - |F_c||/\Sigma|F_o|$; $wR2 = [\Sigma [w(F_o^2 - Fc^2)^2]/ \Sigma[w(F_o^2)^2]]^{1/2}$

Table S4. Crystal data and structure refinement for complex **1I_b** measured at different temperatures.

Identification code	**1I_b**				
CCDC	2060302	2060303	2060301	2060307	2060305
Empirical formula	$C_{26}H_{17}I_2N_3Zn$	$C_{26}H_{17}I_2N_3Zn$	$C_{26}H_{17}I_2N_3Zn$	$C_{26}H_{17}I_2N_3Zn$	$C_{26}H_{17}I_2N_3Zn$
Formula weight	690.59	690.59	690.59	690.59	690.59
Temperature (K)	150(2)	210(2)	240(2)	270(2)	295(2)
Wavelength (Å)	0.71073	0.71073	0.71073	0.71073	0.71073
Crystal system			Monoclinic		
Space group			$P2_1/c$		
Unit cell dimensions					
a (Å)	8.4365(7)	8.4568(3)	8.4628(4)	8.4628(4)	8.4603(4)
b (Å)	21.6792(18)	21.8093(8)	21.8839(10)	21.8839(10)	21.9109(9)
c (Å)	13.4196(11)	13.4962(5)	13.5501(6)	13.5501(6)	13.5774(6)
a (°)	90.000(0)	90.000(0)	90.000(0)	90.000(0)	90.000(0)
β (°)	107.913(2)	107.8530(10)	107.7620(10)	107.7620(10)	107.7070(10)
γ (°)	90.000(0)	90.000(0)	90.000(0)	90.000(0)	90.000(0)
Volume ($Å^3$)	2335.4(3)	2369.33(15)	2389.84(19)	2389.84(19)	2397.64(18)
Z	4	4	4	4	4
ρ_{calc} (Mg/m^3)	1.964	1.936	1.919	1.919	1.913
μ (mm^{-1})	3.715	3.662	3.630	3.630	3.618
F(000)	1320	1320	1320	1320	1320
Crystal size (mm^3)	0.361 × 0.070 × 0.055		0.282 × 0.148 × 0.051		
θ range for data collection (°)	1.851 to 25.997	1.840 to 26.000	1.832 to 25.997	1.832 to 25.997	1.828 to 26.000

Index ranges	-10<=h<=10, -26<=k<=26, -16<=l<=16	-10<=h<=10, -26<=k<=26, -16<=l<=16	-10<=h<=10, -26<=k<=26, -16<=l<=16	-10<=h<=10, -26<=k<=26, -16<=l<=16	-10<=h<=10, -27<=k<=27, -16<=l<=16
Reflections collected	38178	39204	31866	31650	31961
Independent reflections	4609 [R(int) = 0.0472]	4662 [R(int) = 0.0424]	4700 [R(int) = 0.0409]	4700 [R(int) = 0.0454]	4711 [R(int) = 0.0463]
Completeness to θ = 25.242°	100.0 %	100.0 %	100.0 %	100.0 %	100.0 %
Absorption correction	Semi-empirical from equivalents	Numerical	Numerical	Numerical	Numerical
Max. and min. transmission	0.822 and 0.347	0.835 and 0.425	0.837 and 0.428	0.837 and 0.428	0.837 and 0.429
Refinement method	Full-matrix least-squares on F^2				
Data/ restrains/ parameters	4609 / 0 / 289	4662 / 0 / 289	4700 / 0 / 289	4700 / 0 / 289	4711 / 0 / 289
GOOF on F^2	1.024	1.058	1.037	1.025	1. 026
Final R indices [I>2σ(I)][a]	R1 = 0.0351, wR2 = 0.0783	R1 = 0.0325, wR2 = 0.0704	R1 = 0.0341, wR2 = 0.0737	R1 = 0.0348, wR2 = 0.0778	R1 = 0.0373, wR2 = 0.0845
R indices (all data)	R1 = 0.0450, wR2 = 0.0816	R1 = 0.0423, wR2 = 0.0741	R1 = 0.0464, wR2 = 0.0784	R1 = 0.0511, wR2 = 0.0836	R1 = 0.0550, wR2 = 0.0903
Largest diff. peak and hole (e.Å^{-3})	2.910 and -0.718	2.415 and -0.837	2.439 and -0.992	2.260 and -1.027	2.249 and -0.956

[a] $R_1 = \Sigma||F_o| - |F_c||/\Sigma|F_o|$; $wR2 = [\Sigma [w(F_o^2 - Fc^2)^2]/ \Sigma[w(F_o^2)^2]]^{1/2}$

Table S5. Selected bond lengths and angles for complexes **1I**, **1Cl**, **1OAc**, **2Cl**, **2I**, **3OAc_y**.

	1I_a	**1Cl_a**	**1Cl_b**	**1OAc**	**2Cl**	**2I**	**3OAc_y**
				Bond lengths, Å			
Zn–N(1)	2.024(2)	2.0161(14)	2.024(2)	2.0847(17)	2.019(4)	2.055(4)	2.090(5)
Zn–N(2)	2.075(3)	2.0548(15)	2.075(2)	2.0532(17)	2.062(4)	2.064(4)	2.059(5)
Zn–Cl(1)	-	2.2157(5)	2.2167(6)	-	2.2077(16)	–	-
Zn–Cl(2)	-	2.2069(5)	2.2018(7)	-	2.2135(16)	–	-
Zn–I(1)	2.5392(4)	-	-	-	-	2.5638(7)	-
Zn–I(2)	2.5469(5)	-	-	-	-	2.5368(7)	-
				Bond angles, °			
N(1)–Zn–N(2)	80.75(10)	81.16(6)	80.73(7)	80.73(7)	80.69(17)	80.42(16)	79.8(2)
Cl(2)–Zn–Cl(1)	-	116.64(2)	118.76(3)	-	116.83(6)		-
I(2)–Zn–I(1)	119.672(16)	-	-	-	–	120.74(2)	-
O–Zn–O	–	–	–	107.14(7)	–	–	105.9(3)

Table S6. Selected bond lengths and angles for **1I_b** at different temperatures.

	150 K	**210K**	**240K**	**270K**	**295K**
			Bond lengths, Å		
Zn–N(1)	2.037(4)	2.046(3)	2.049(3)	2.046(3)	2.041(3)
Zn–N(2)	2.068(4)	2.081(3)	2.082(4)	2.081(4)	2.083(4)
Zn–I(1)	2.5468(6)	2.5434(6)	2.5517(6)	2.5418(6)	2.5405(6)
Zn–I(2)	2.5358(6)	2.5497(6)	2.5482(6)	2.5474(6)	2.5443(7)
			Bond angles, °		
N(1)–Zn–N(2)	80.12(14)	80.15(13)	80.06(14)	80.12(14)	80.01(15)
I(2)–Zn–I(1)	110.70(2)	110.78(2)	110.83(2)	110.95(2)	111.05(2)

Table S7. Intermolecular separation (d I···π_{imi}), the ratio of intensities of the phosphorescence and fluorescence bands (I_p / I_f), observed lifetime of the phosphorescence, and CIE 1931 chromaticity coordinates of the emission for **1I_b** at different temperatures.

***T*, K**	***d* (I···π_{imi}), Å**	I_p / I_f	τ_{obs} **(600 nm), ns**	***CIE* (*x*, *y*)**
295	3.572	0.39	0.09×10^6	0.222, 0.249
270	3.562	0.44	0.1×10^6	0.225, 0.252
230	–	1.12	0.5×10^6	0.312, 0.311
240	3.547	–	–	–
210	3.531	–	–	–
190	–	2.24	1.3×10^6	0.382, 0.360
150	3.499	2.62	1.9×10^6	0.394, 0.371
110	–	2.85	2.1×10^6	0.396, 0.376
77	–	2.85	2.2×10^6	0.393, 0.376

Table S8. Emission wavelengths of zinc complexes in solid state before and after mechanical grinding at 298 K.

complex	**λ_{ems}, nm**	
	pristine crystals	**ground sample**
2Cl	472	532
2I	506, 598	500, 534, 583 494, 524, 573 (drop-cast)
2OAc	497	515
L3_y	543	575 598 after heatig/vapors
L3_r	597	564
3OAc_r	611	563

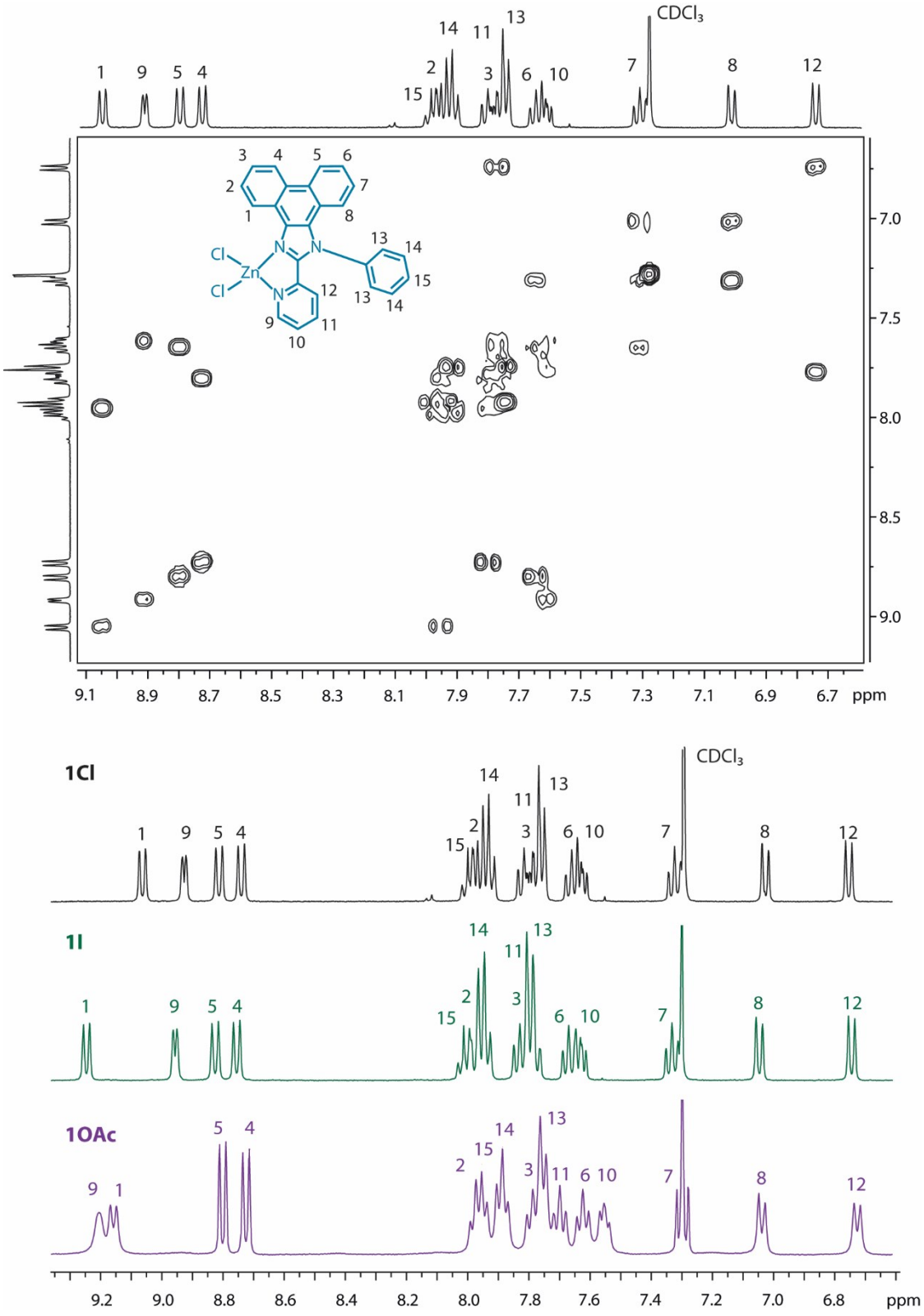

Figure S1. ^{1}H NMR spectra of complexes **1X** in the aromatic region (400 MHz, $CDCl_3$, 298 K).

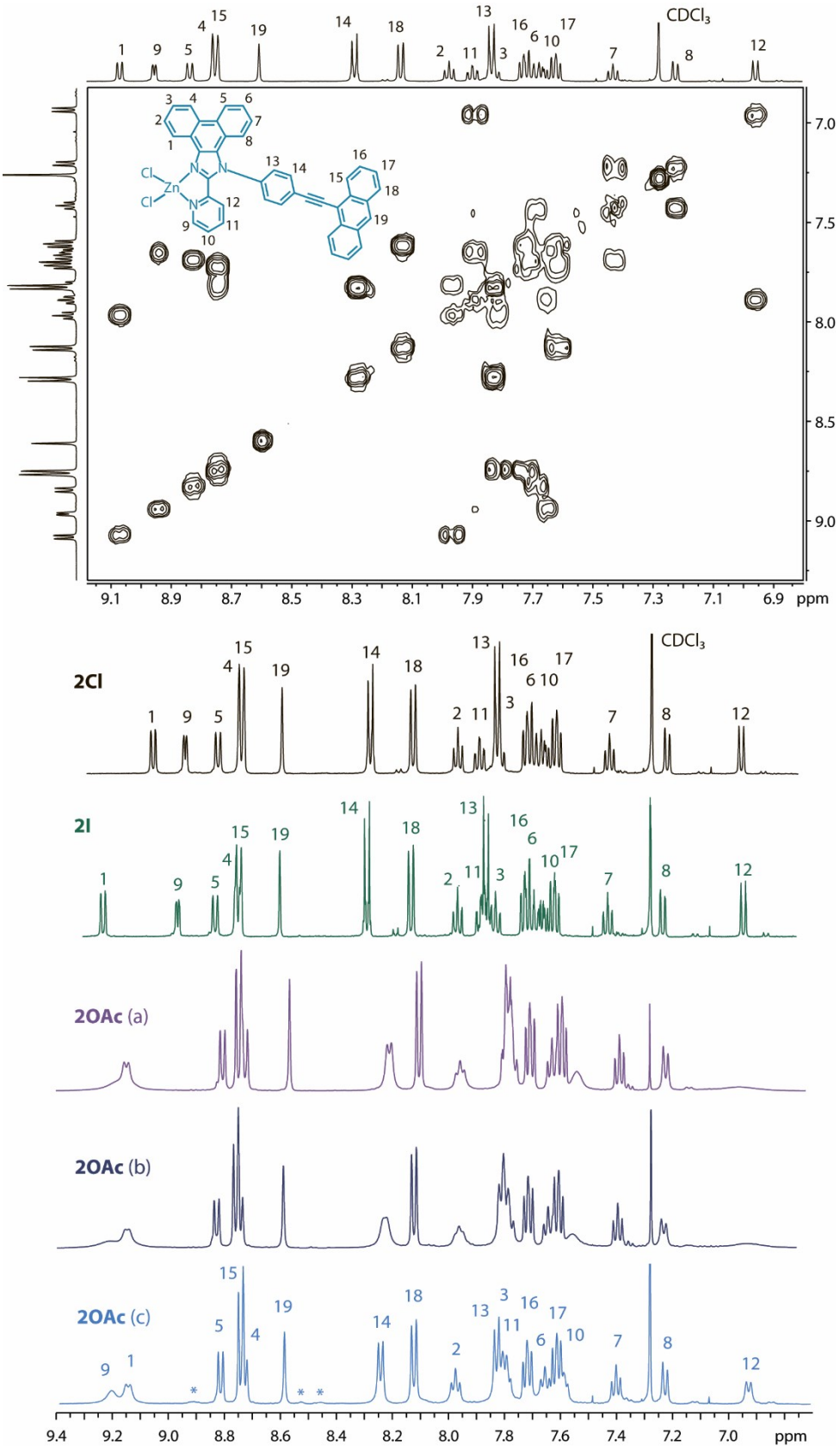

Figure S2. ^{1}H NMR spectra of complexes **2Cl**, **2I** and of **2OAc** with various concentrations (a: 57.9 mmol/L; b: 18.1 mmol/L; c: 3.63 mmol/L, asterisks denote broadened signals assigned to the free **L2**) in the aromatic region (500 MHz, $CDCl_3$, 298 K).

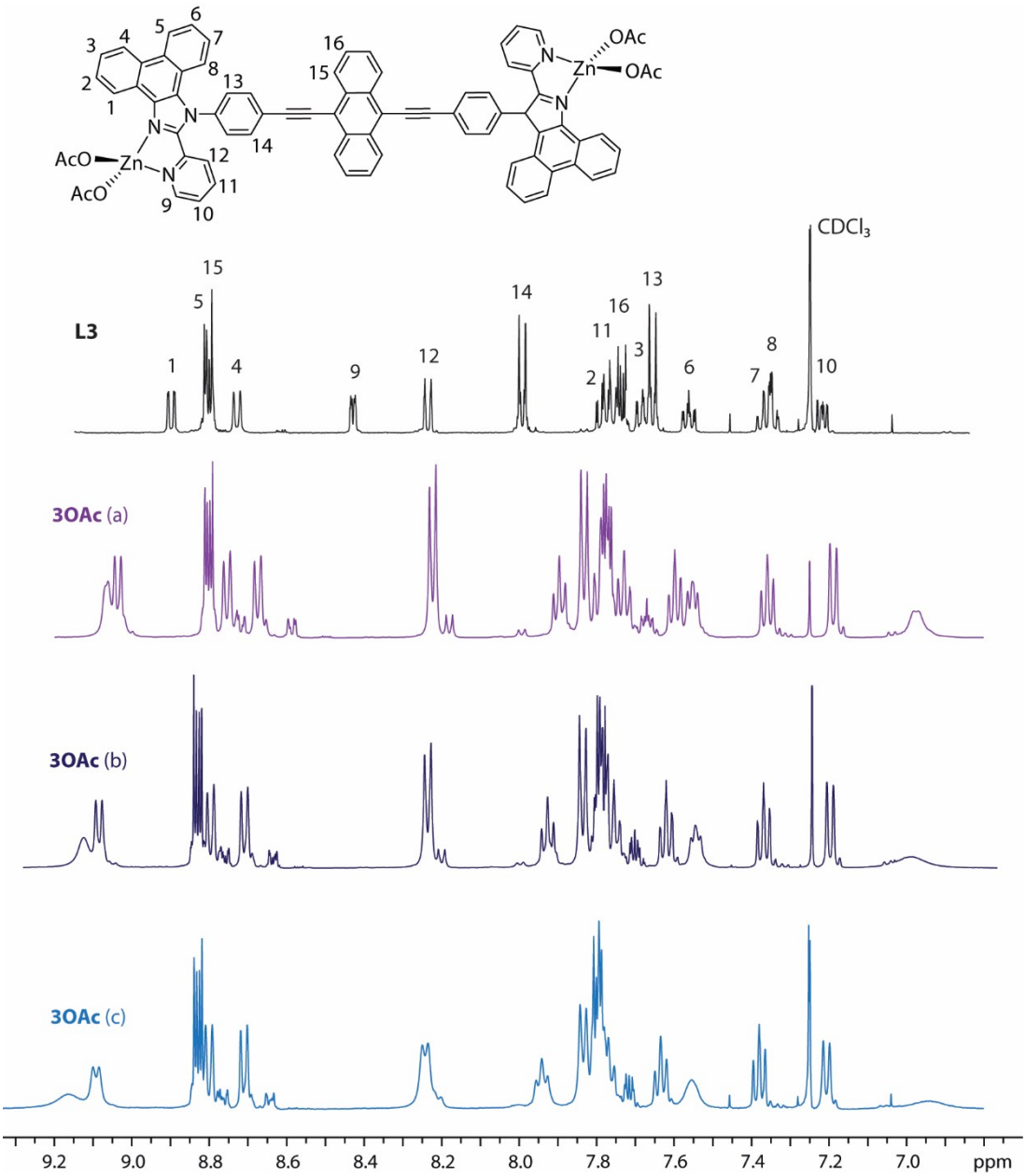

Figure S3. ^{1}H NMR spectra of ligand **L3** and of complex **3OAc** at different concentrations (a: 8.5 mmol/L; b: 1.8 mmol/L; c: 0.42 mmol/L) in the aromatic region (500 MHz, $CDCl_3$, 298 K).

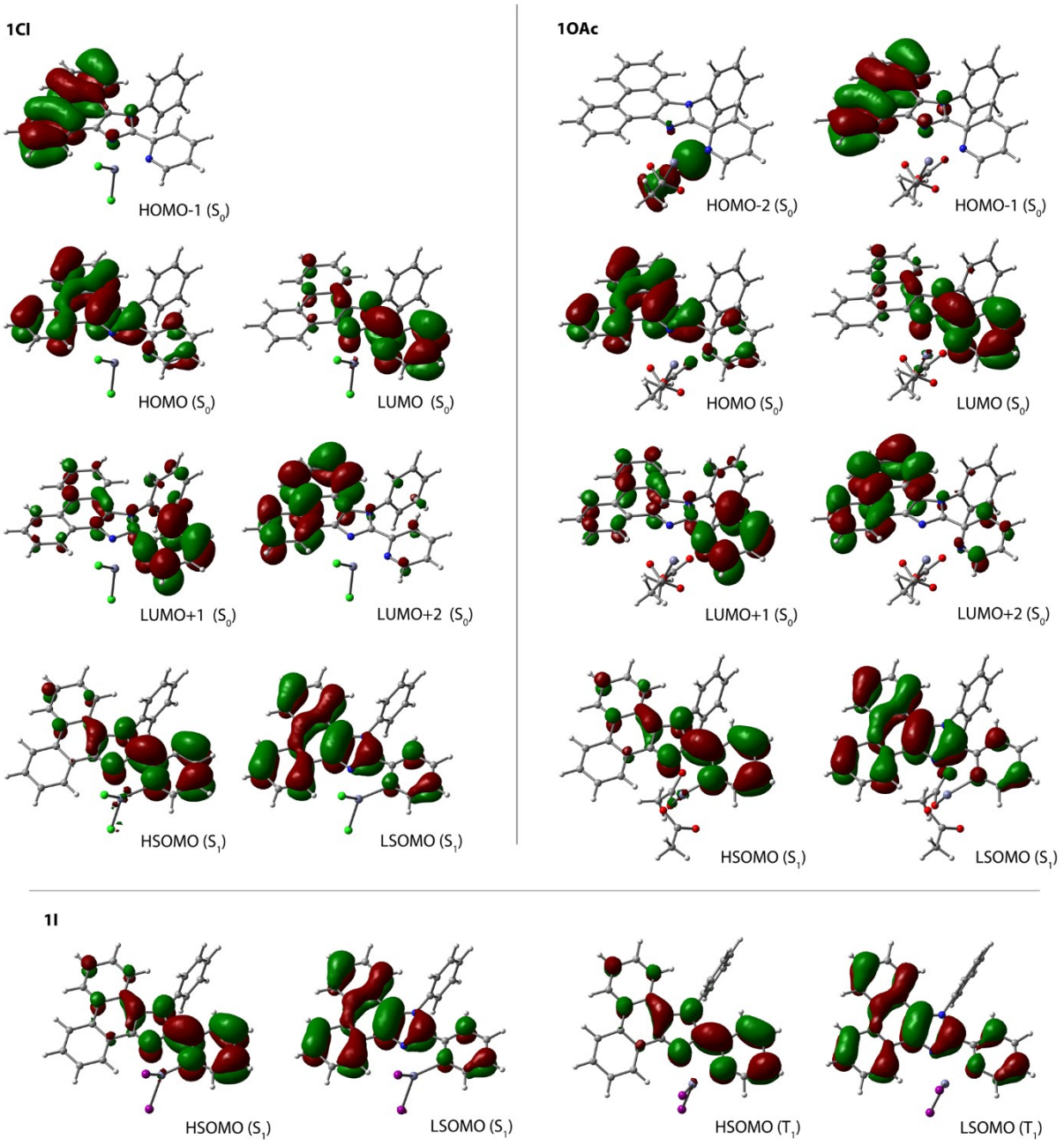

Figure S4. Frontier molecular orbitals for the ground and the lowest excited states of complexes **1Cl**, **1OAc** and **1I**.

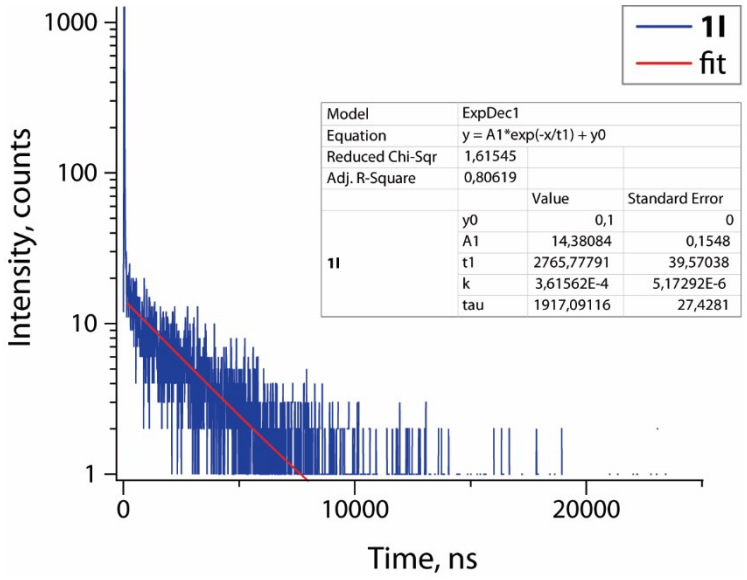

Figure S5. Decay profile for long live band for complex **1I** monitored at 560 nm (degassed 1,2-dichloroethane, 298 K, $c = 10^{-5}$ M, $\lambda_{exc} = 351$ nm).

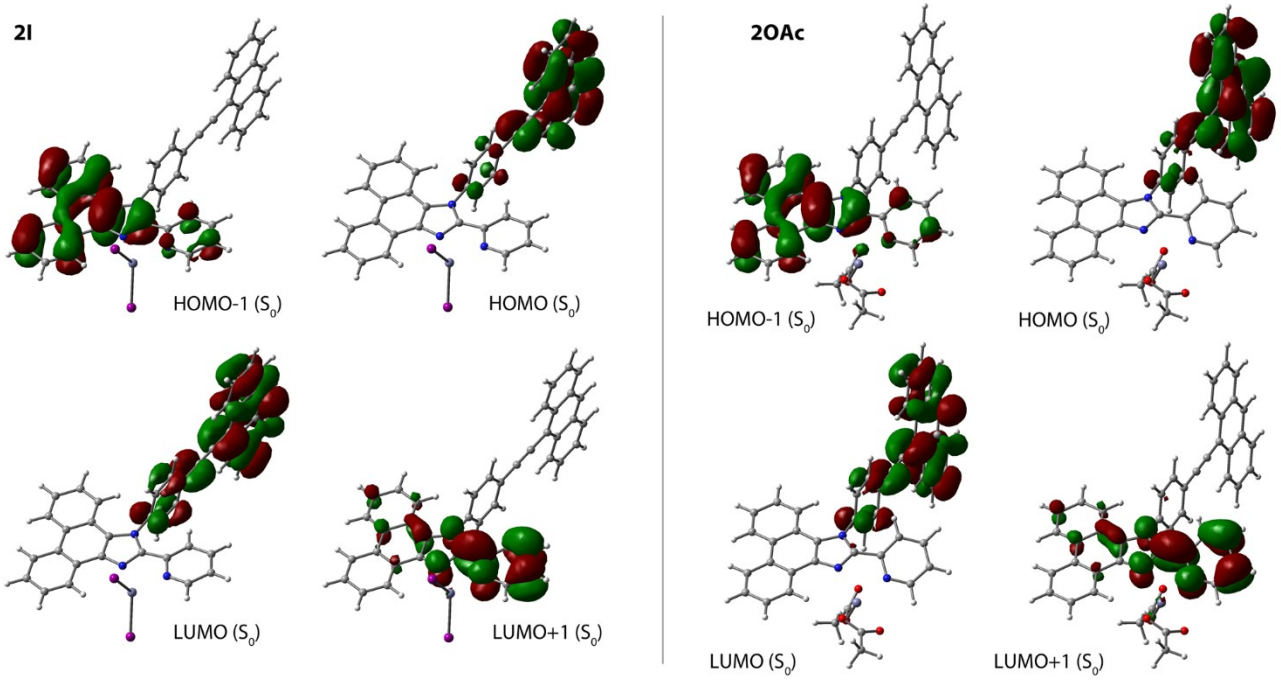

Figure S6. Frontier molecular orbitals for complexes **2I** and **2OAc**.

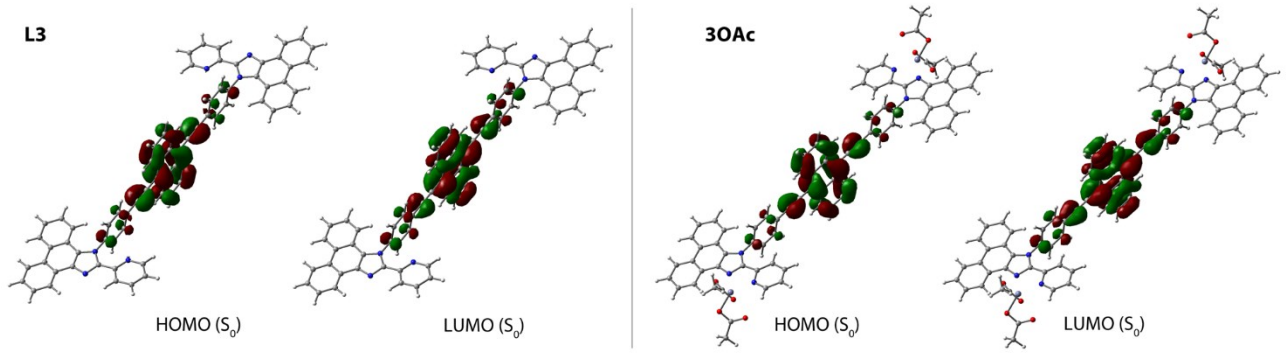

Figure S7. Frontier molecular orbitals for ligand **L3** and complex **3OAc**.

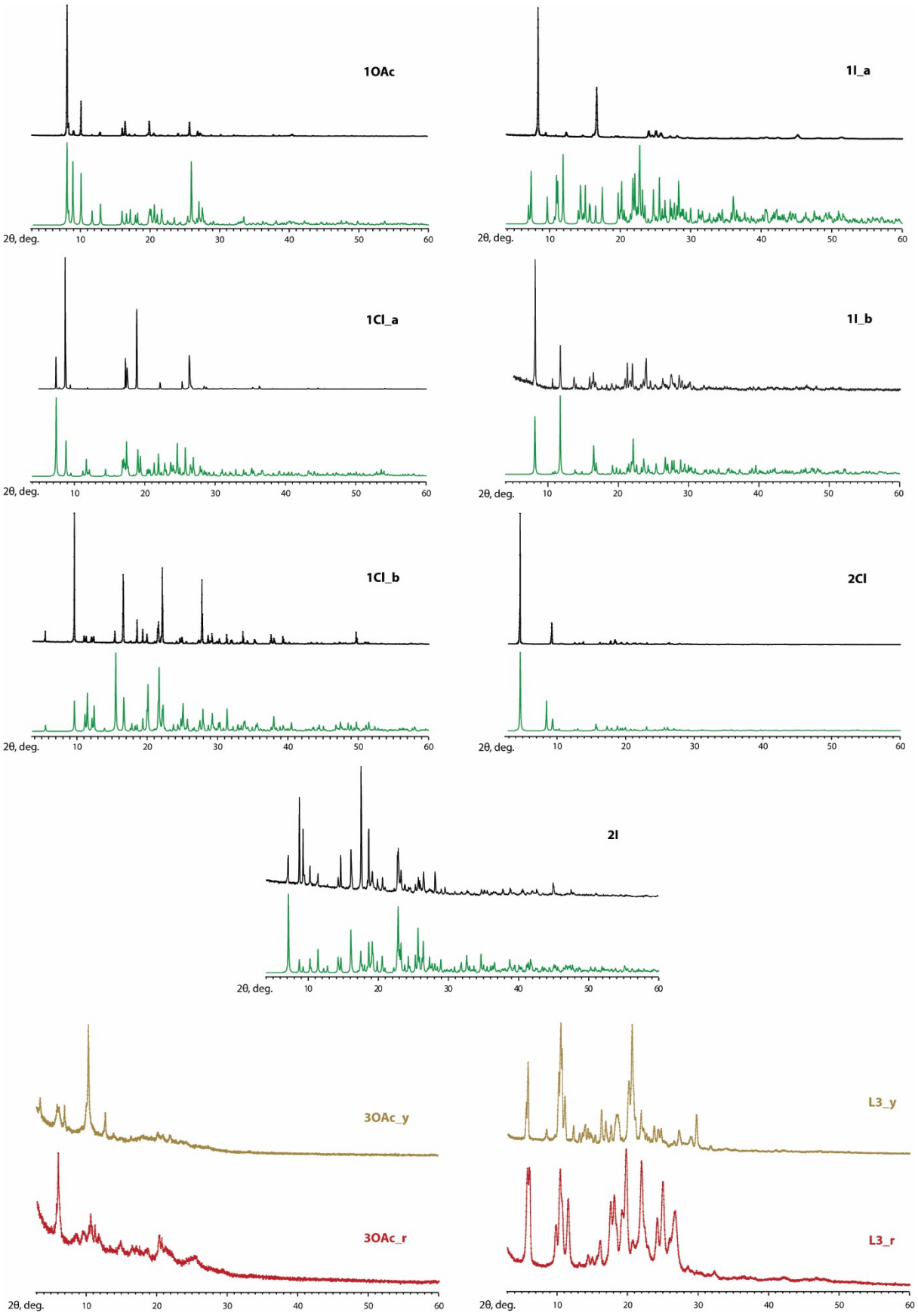

Figure S8. Powder XRD patterns for dried crystals of **1OAc**, **1Cl_a/b**, **1I_a/b**, **2Cl**, **2I** (green traces: simulated from single crystal data, black traces: experimental), **L3** and **3OAc** (yellow and red forms). The differences between the experimental and simulated diffractograms are attributed to the loss of crystallization solvent and the accompanying phase changes.

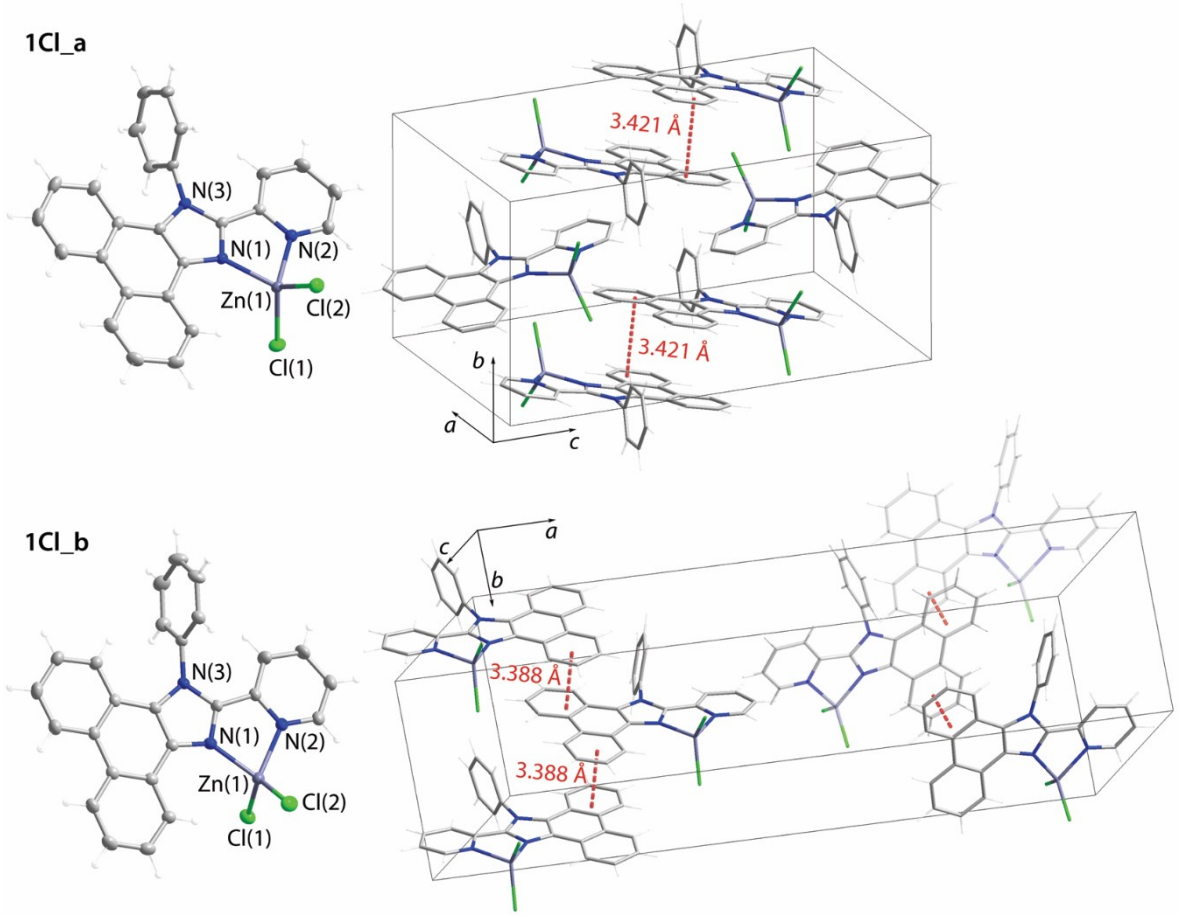

Figure S9. Molecular views and packing fragment (partial filling for **1Cl_b**) for dichloromethane and chloroform solvates **1Cl_a** (top) and **1Cl_b** (bottom). The intermolecular π–π distances were measured between the planes of the phenanthrene motifs. Crystallization solvent molecules are omitted for clarity. Thermal ellipsoids are shown at the 50% probability level.

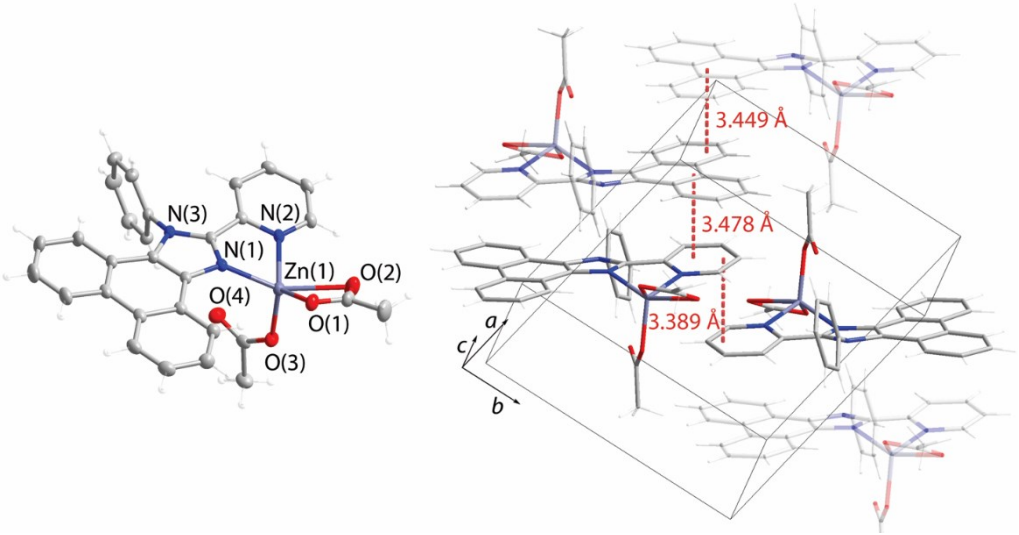

Figure S10. Molecular view and packing fragment for **1OAc**. Crystallization water molecules are omitted for clarity. Thermal ellipsoids are shown at the 50% probability level.

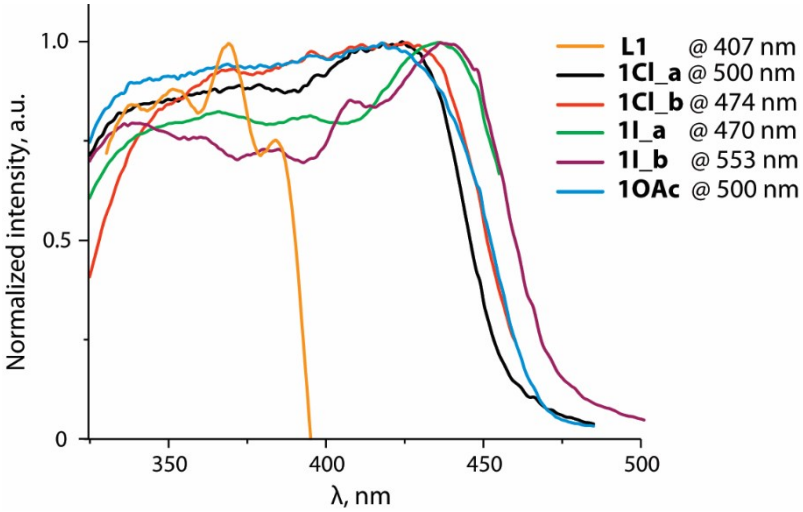

Figure S11. Normalized solid state excitation spectra for **L1** and the corresponding zinc(II) complexes **1X** at 298 K.

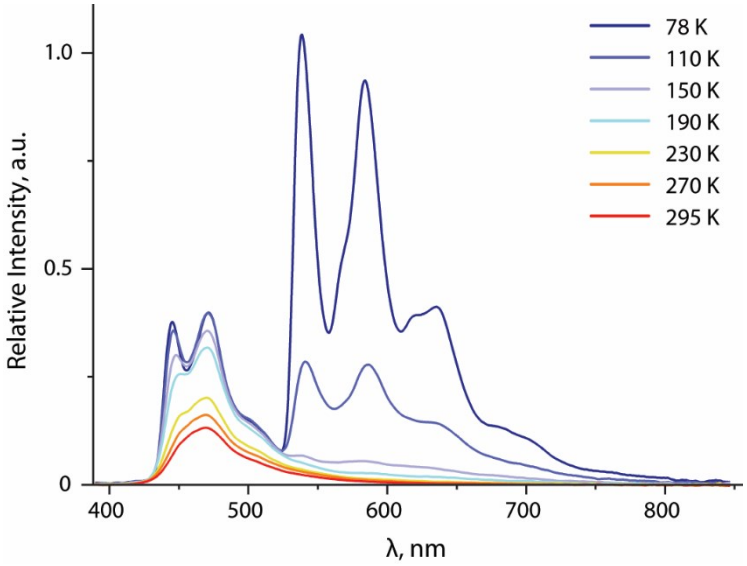

Figure S12. Variable temperature solid state emission spectra for **1I_a**.

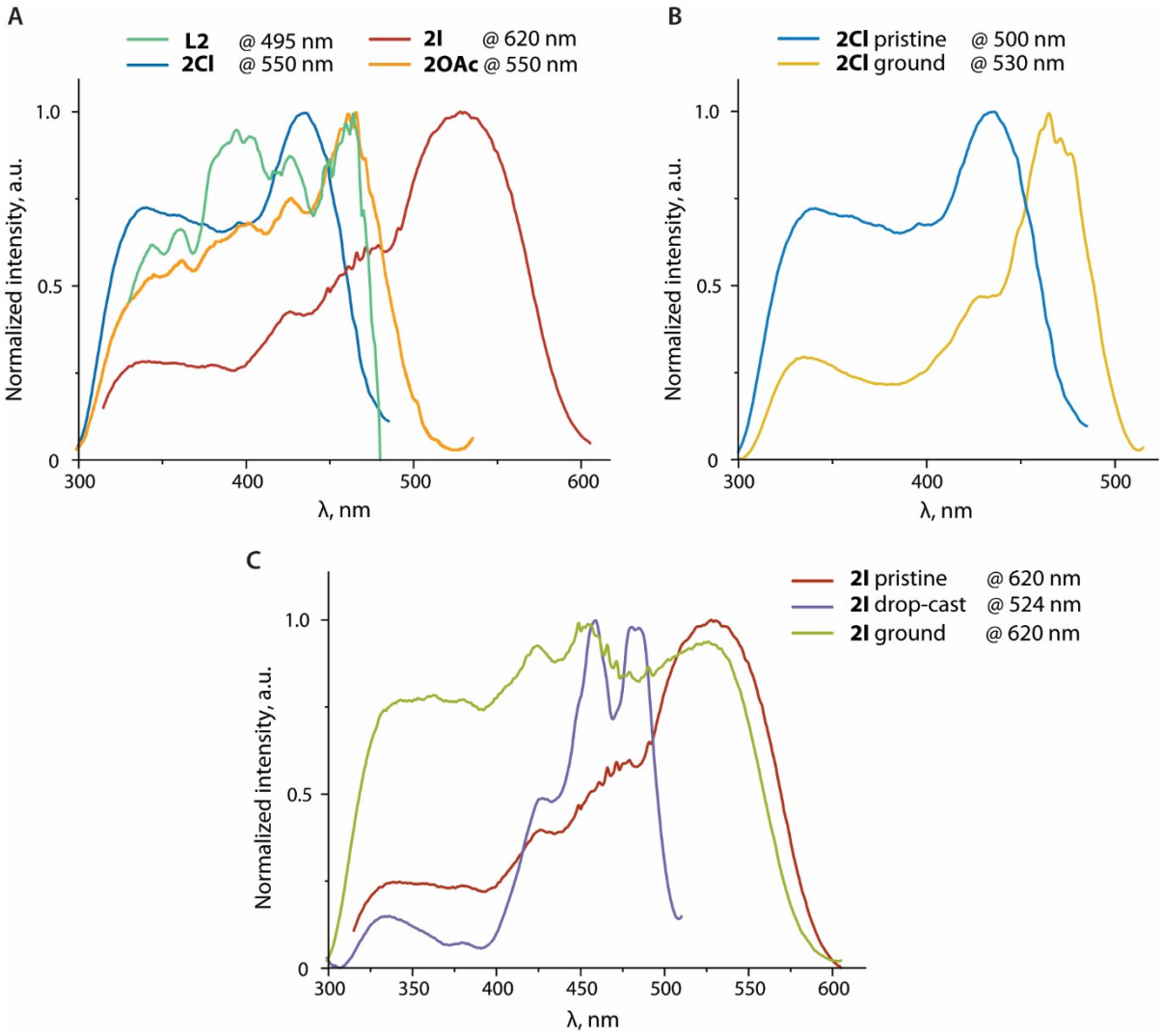

Figure S13. Normalized solid state excitation spectra for **L2** and the corresponding zinc(II) complexes **2X** at 298 K.

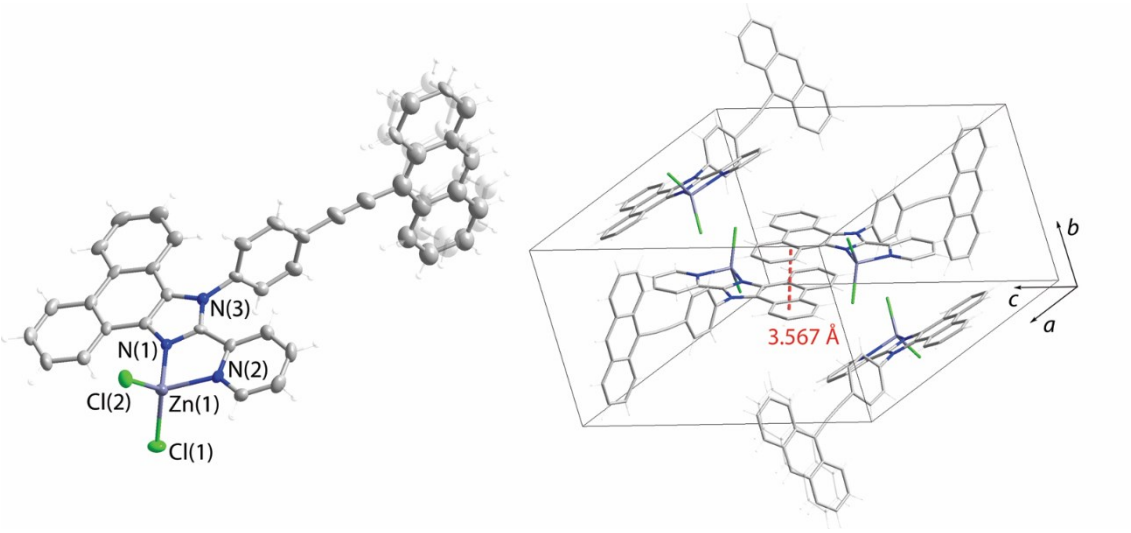

Figure S14. Molecular view and unit cell packing for **2Cl**. Two components of the disordered anthracene motif are shown. Crystallization solvent was disordered and omitted from the refinement model. The intermolecular π–π distances were measured between the planes of the phenanthrene motifs. Thermal ellipsoids are shown at the 50% probability level.

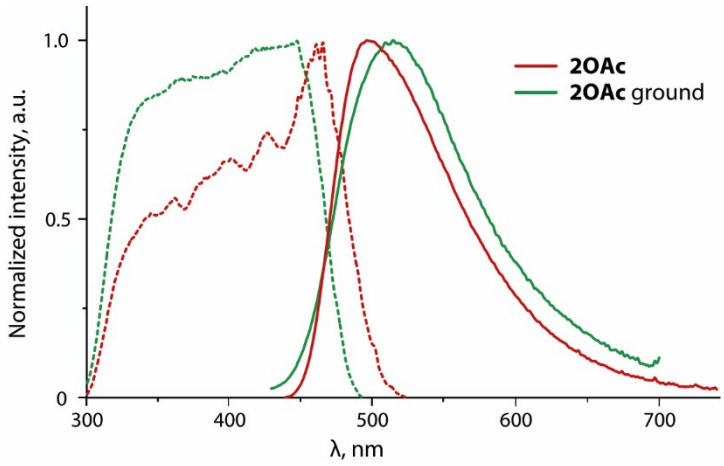

Figure S15. Normalized solid state excitation (dashed lines) and emission (solid lines) spectra for pristine and ground samples of complex **2OAc** at 298 K.

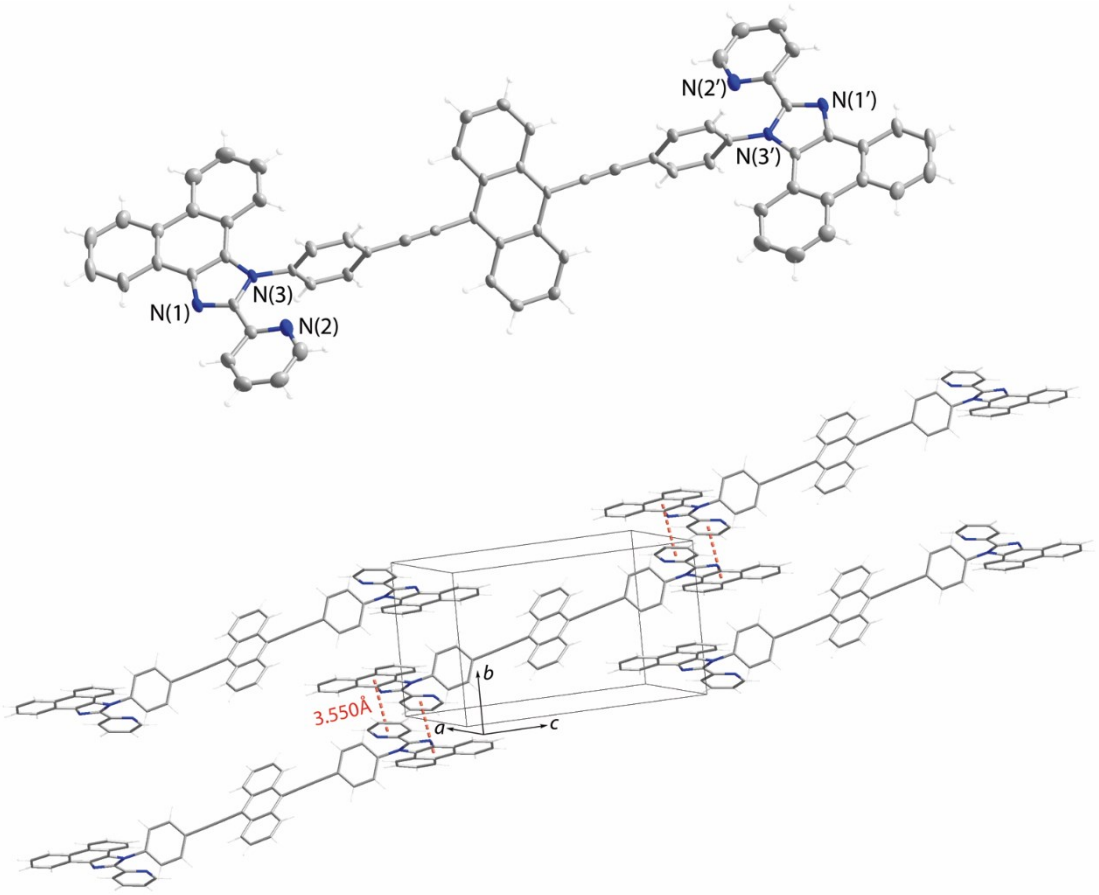

Figure S16. Molecular view and packing fragment for **L3_y$_{cr}$**. Crystallization solvent was disordered and omitted from the refinement model. The intermolecular π–π distances were measured between the centroids of the phenanthrene and pyridine rings. Symmetry transformations used to generate equivalent atoms (′): 1–x, 1–y, 1–z. Thermal ellipsoids are shown at the 50% probability level.

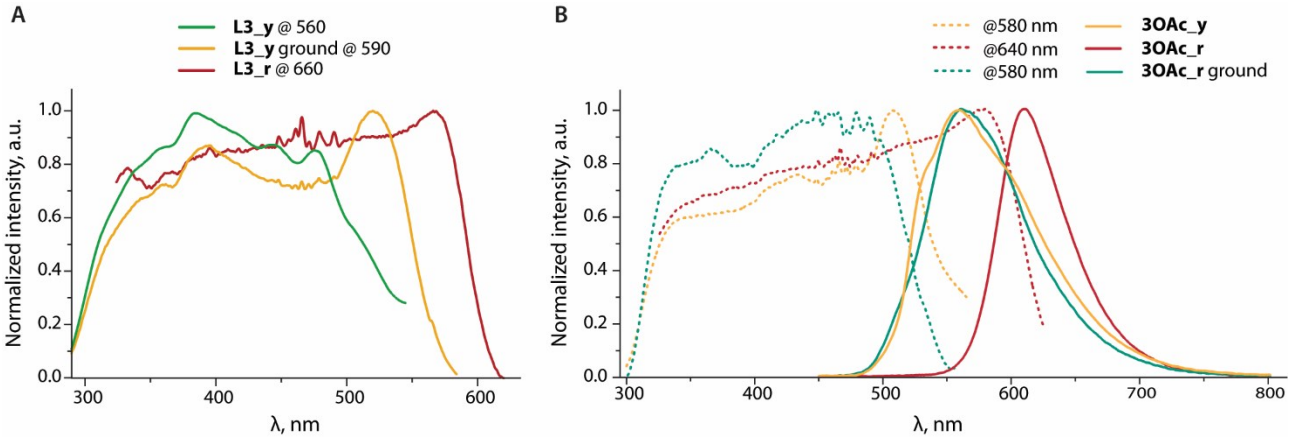

Figure S17. Normalized solid state excitation spectra for **L3** and the corresponding zinc(II) complex **3OAc** at 298 K.

References

1. Cakmak, O.; Erenler, R.; Tutar, A.; Celik, N., *J. Org. Chem.* **2006,** *71*, 1795-1801.

2. Kisel, K. S.; Eskelinen, T.; Zafar, W.; Solomatina, A. I.; Hirva, P.; Grachova, E. V.; Tunik, S. P.; Koshevoy, I. O., *Inorg. Chem.* **2018,** *57*, 6349−6361.

3. *APEX2 - Software Suite for Crystallographic Programs*, Bruker AXS, Inc.: Madison, WI, USA, 2010.

4. Sheldrick, G. M. *SADABS-2008/1 - Bruker AXS Area Detector Scaling and Absorption Correction*, Bruker AXS: Madison, Wisconsin, USA, 2008.

5. Sheldrick, G. M., *Acta Crystallogr. C: Struct. Chem.* **2015,** *71*, 3-8.

6. Farrugia, L. J., *J. Appl. Crystallogr.* **2012,** *45*, 849–854.

7. Spek, A. L., *Acta Cryst.* **2015,** *C71*, 9–18.

8. Spek, A. L. *PLATON, A Multipurpose Crystallographic Tool*, 1.17; Utrecht University: Utrecht, The Netherlands, 2013.

9. Brouwer, A. M., *Pure & Appl. Chem.* **2011,** *83*, 2213–2228.

10. Frisch, M. J.; Trucks, G. W.; Schlegel, H. B.; Scuseria, G. E.; Robb, M. A.; Cheeseman, J. R.; Scalmani, G.; Barone, V.; Petersson, G. A.; Nakatsuji, H.; Li, X.; Caricato, M.; Marenich, A. V.; Bloino, J.; Janesko, B. G.; Gomperts, R.; Mennucci, B.; Hratchian, H. P.; Ortiz, J. V.; Izmaylov, A. F.; Sonnenberg, J. L.; Williams-Young, D.; Ding, F.; Lipparini, F.; Egidi, F.; Goings, J.; Peng, B.; Petrone, A.; Henderson, T.; Ranasinghe, D.; Zakrzewski, V. G.; Gao, J.; Rega, N.; Zheng, G.; Liang, W.; Hada, M.; Ehara, M.; Toyota, K.; Fukuda, R.; Hasegawa, J.; Ishida, M.; Nakajima, T.; Honda, Y.; Kitao, O.; Nakai, H.; Vreven, T.; Throssell, K.; Montgomery, J. A. J.; Peralta, J. E.; Ogliaro, F.; Bearpark, M. J.; Heyd, J. J.; Brothers, E. N.; Kudin, K. N.; Staroverov, V. N.; Keith, T. A.; Kobayashi, R.; Normand, J.; Raghavachari, K.; Rendell, A. P.; Burant, J. C.; Iyengar, S. S.; Tomasi, J.; Cossi, M.; Millam, J. M.; Klene, M.; Adamo, C.; Cammi, R.; Ochterski, J. W.; Martin, R. L.; Morokuma, K.; Farkas, O.; Foresman, J. B.; Fox, D. J. *Gaussian 16*, Revision A.03; Gaussian, Inc.: Wallingford CT, 2016.

11. Adamo, C.; Barone, V., *J. Chem. Phys.* **1999,** *110*, 6158-6170.

12. Grimme, S.; Antony, J.; Ehrlich, S.; Krieg, H., *J. Chem. Phys.* **2010,** *132*, 154104.

13. Grimme, S.; Ehrlich, S.; Goerigk, L., *J. Comput. Chem.* **2011,** *32*, 1456-1465.

14. Rappoport, D.; Furche, F., *J. Chem. Phys.* **2010,** *133*, 134105.

15. Barone, V.; Cossi, M., *J. Phys. Chem. A* **1998,** *102*, 1995–2001.

16. Cossi, M.; Rega, N.; Scalmani, G.; Barone, V., *J. Comput. Chem.* **2003,** *24*, 669–681.